ELSEVIER

Journal of Crystal Growth 218 (2000) 87–92

JOURNAL OF CRYSTAL GROWTH

www.elsevier.nl/locate/jcrysgro

The growth defects in Czochralski-grown Yb : YAG crystal

Yang Peizhi[a,*], Deng Peizhen[b], Yin Zhiwen[a], Tian Yulian[c]

[a]*Laboratory of Functional Inorganic Materials, Shanghai Institute of Ceramics, Chinese Academy of Sciences, Shanghai 200050, People's Republic of China*

[b]*Shanghai Institute of Optics and Fine Mechanics, Chinese Academy of Sciences, Shanghai 201800, People's Republic of China*

[c]*Beijing Synchrotron Radiation Laboratory, Institute of High Energy, Chinese Academy of Sciences, Beijing 100039, People's Republic of China*

Received 11 April 2000; accepted 17 April 2000

Communicated by M. Schieber

Abstract

The growth defects in Yb : YAG crystals were investigated by transmission synchrotron topography and chemical etching. The etch pit patterns on three low-index planes (1 1 1), (1 1 0) and (2 1 1) were obtained. It was found that growth striations, core and dislocations were the main defects in Yb : YAG crystal. The dislocations in Yb : YAG mainly originated from seed, impurity particles and inclusions, and seed–crystal interfaces in the initial growth period. The dislocations usually propagate along a path perpendicular to the growth interface. Therefore, in Yb : YAG crystals grown with a convex solid–liquid interface, the dislocations will be decreased or eliminated.

PACS: 61.72.Ff; 61.72.Cc

Keywords: Yb : YAG; Defects; Transmission synchrotron topography; Chemical etching; Dislocations

1. Introduction

Recently, with the development of InGaAs laser diode [1], Yb^{3+}-doped solid-state materials are attractively used as gain media for high-efficiency, high-power laser diode-pumped laser systems. Among the numerous Yb-doped oxide and fluoride crystals, Yb : YAG crystal plays an important role [2] since it possesses many attractive characteristics, including high thermal conductivity and tensile strength of the host material, small quantum defect between the pump and the laser photons resulting in low thermal loading, broad absorption bands (about 18 nm at 940 nm), long radiative lifetime of the upper laser level (1.3 ms). Therefore, the spectroscopic and laser performances of Yb : YAG have been intensively and systematically investigated [3–5]. However, the study on its growth defects has not been performed until now. It is well known that the perfection of laser crystals is one of the most important performances. The defects in laser crystals influence the optical homogeneity and deteriorate the laser output characteristics. Thus, it is necessary to study the defects of Yb : YAG.

* Corresponding author. Fax: + 86-021-625-13903.

E-mail address: pzhyang@mail.sic.ac.cn (Yang Peizhi).

0022-0248/00/$ - see front matter
PII: S0022-0248(00)00531-5

In this paper, we report the investigation on growth defects in 20 at% Yb : YAG by transmission synchrotron topography and chemical etching which is helpful for the crystal grower to improve the quality of Yb : YAG crystals.

2. Experiment

2.1. Crystal growth

The Yb : YAG crystal with a Yb^{3+} doping level of 20 at% used in the experiment was grown by the CZ method with the [1 1 1] seeding orientation, and the detailed growth parameters are demonstrated in Ref. [6]. The crystal boule was 33 mm in diameter and 110 mm in length.

2.2. Chemical etching

Three kinds of crystal slices with [1 1 1], [2 1 1] and [1 1 0] orientation were cut from the as-grown crystal boule and the slices were subsequently polished on both sides with diamond paste. The mechanically polished slices were chemically polished in liquid H_3PO_4 at 320°C for 20 min, then etched in liquid H_3PO_4 at 250–260°C for 10 min. Etch pits of dislocations with different low-index planes were observed under the optical microscope.

2.3. Transmission synchrotron topography

The slices parallel to the (1 1 0) planes, which include the [1 1 1] growth axis and the slices parallel to the (1 1 1) planes, which are perpendicular to the [1 1 1] growth axis were chosen for cutting from 20 at% Yb : YAG crystal. The slices were mechanically polished to 0.2 mm. The samples were then chemically polished in liquid H_3PO_4 at 320°C for 30 min to be thinned to 0.1 mm and to remove the residual strain. The transmission synchrotron topographs were obtained at Beijing Synchrotron Radiation Laboratory. The topographs were taken with a white-beam topography camera and recorded on Fuji films.

3. Results and discussion

3.1. The etch pit patterns on three low-index planes (1 1 1), (1 1 0) and (2 1 1)

The etch pit patterns can be formed after chemical etching. Generally, the symmetry of an etch pit is in accordance with the symmetry of the crystal face, and the shapes of etch pits on different faces are different for the same crystal [7]. The change of etching conditions may also affect etch-pit morphology. Distribution of dislocations in crystals can be determined by observing the etch pits.

Figs. 1A–C are the typical etch pits produced on (1 1 1), (2 1 1) and (1 1 0) face on the upper part of 20 at% Yb : YAG crystal boule. The etch pits can be grouped into five categories: (1) dislocation cluster originating from impurity ions and inclusions; (2) dislocation pits array; (3) single dislocation pit; (4) terraced pits, which may be associated with the change of Yb^{3+} segregation concentration around a dislocation; (5) the accumulation with two or more dislocation pits corresponding to dislocation lines. Under the same etching conditions, the pits on (1 1 1) face have two shapes, one is triangular, and the other is six-sided. The pit pattern on (2 1 1) is triangular with a tail and the pit pattern on (1 1 0) is a distorted rhombus. For (1 1 1) slices, more etch pits can be observed in the initial growth period, which implies that the crystal is imperfect, and with an increase of distance from the seed the number of pits decreases gradually and they are mainly centered at the periphery of the sections. In the middle parts of Yb : YAG crystal, there were only few etch pits, which implies that the crystal is perfect.

The overall dislocation density of about $100\,cm^{-2}$ was revealed by chemical etching technique. In the upper parts of the crystal, the dislocation density is much higher than the average density, and in the middle parts, the dislocation density is nearly zero. These experimental results can be attributed to the ionic radius of Yb^{3+} (0.985 Å) which is close to that of Y^{3+} (1.019 Å) [8] which results in only a little difference of the lattice constant between YbAG and YAG [9].

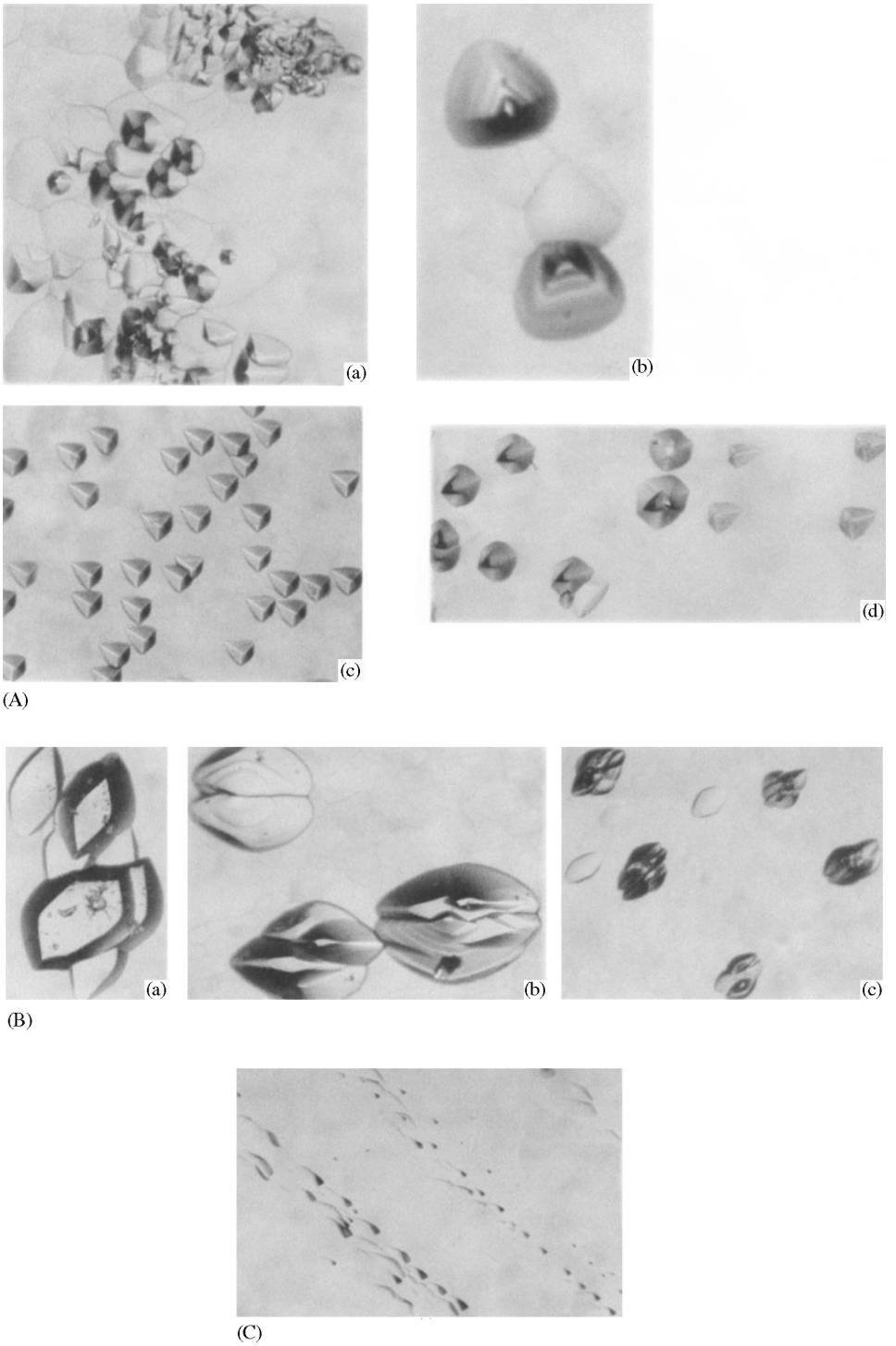

Fig. 1. (A) Etch pit patterns formed on (1 1 1) faces of 20 at% Yb : YAG (a), (c), (d) – (× 250); (b) – (× 500). (B) Etch pit patterns formed on (1 1 0) faces of 20 at% Yb : YAG (a), (b) – (× 250); (c) – (× 100). (C) Etch pit patterns formed on (2 1 1) face of 20 at% Yb : YAG (× 250).

3.2. The defects in Yb : YAG

Fig. 2 shows the transmission synchrotron topography of a (1 1 0) slice of 20 at% Yb : YAG crystal with (1 2 1) reflection displaying typical growth defects in Yb : YAG. Growth striations can be clearly seen on the topograph, which represent the history of crystal growth and the shape and change of the solid–liquid (S/L) interface. The topography shows that the S/L interface is convex towards the melt. The formation of striations is mainly due to the fluctuation of growth parameters. The strong stress field of striae can promote the precipitation of impurity ions. The striations in topography can be classified into two categories: one is darker in contrast and the striations are thick, which is caused by melt flux. The other striations are thin and dense, which is generated by the rotation of crystal and the fluctuation of temperature. The striations also show the deviation degree of the temperature field; near the center of the temperature field the distance between striations is wide, and far from the center the distance is narrow. The growth striations can be reduced through optimizing growth parameters, but they are not eliminated even when they are annealed at 1600°C for 36 h in oxygen atmosphere.

Figs. 2a–c also demonstrate dislocation bundles and dislocation lines towards the crystal periphery in the upper parts of the Yb : YAG crystal. However, in the middle parts of Yb : YAG crystal, they vanish, as shown in Fig. 2d. These experimental results are in good agreement with those obtained by chemical etching.

Fig. 3 shows the transmission synchrotron topographs of a (1 1 1) slice of 20 at% Yb : YAG with (2 1 0) reflection. Only a part of the whole slice is presented in Fig. 3a due to the limit of the area of the light source. Core and side core can be clearly seen in the topograph, which is a large stress center. Core and side core are the characteristics of rare-earth doped YAG grown along the [1 1 1] direction with convex growth interface. The core is formed by three {2 1 1} facet planes and {1 1 0} facet planes, and the side core is formed by three {2 1 1} facet planes. Generally speaking, rare-earth doped YAG crystals grown along the [1 1 1] direction have the smallest core and show good laser performances. The difference of temperature field and Yb^{3+} segregation induce a small difference in the refractive index, lattice parameters, stress and Yb^{3+} doping level between the core and the other region. The Yb^{3+} concentration is 5% higher in the core area than in the other areas for 20 at% Yb : YAG crystal, which was determined by measuring the absorption

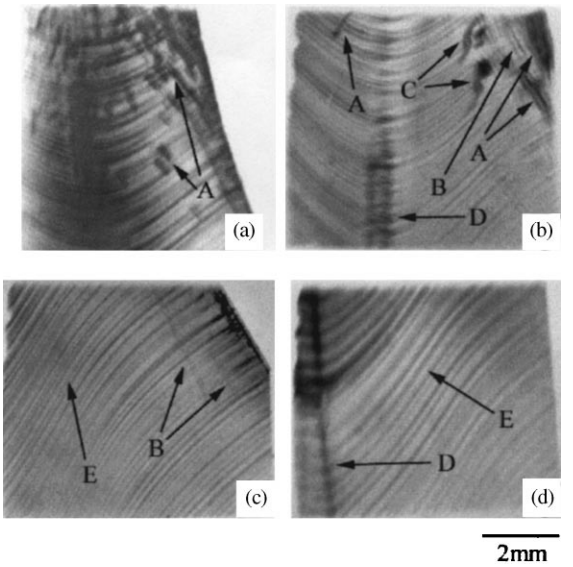

Fig. 2. The transmission synchrotron topography of (1 1 0) slices of 20 at% Yb : YAG parallel to the [1 1 1] growth axis with (1 2 1) reflection. (a) → (b) → (c) → (d): from the upper parts to the middle of the crystal. (A) dislocation bundles originated from seed–crystal interfaces; (B) dislocation lines; (C) dislocation bundles originating from impurity or inclusions; (D) core and side core; (E) growth striations.

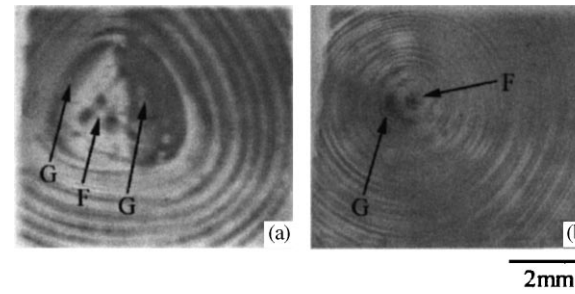

Fig. 3. The transmission synchrotron topography of (1 1 1) slices of 20 at% Yb : YAG perpendicular to the [1 1 1] growth axis with (2 1 0) reflection. (a) as-grown crystal; (b) annealed crystal at 1600°C for 36 h. (F) core; (G) side core.

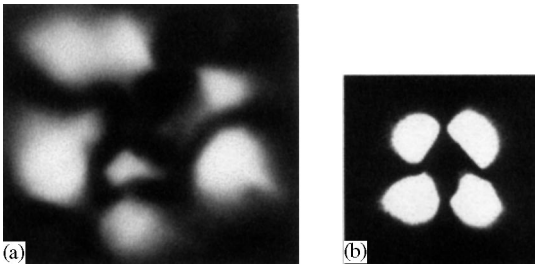

Fig. 4. Stress-birefringence of 20 at% Yb:YAG in a section perpendicular to [1 1 1]. (a) As-grown crystal; (b) annealed crystal at 1600°C for 36 h.

spectrum at 850–1150 nm. The core area was large in the as-grown 20 at% Yb:YAG boule, after being annealed at 1600°C for 36 h in oxygen atmosphere the core area was reduced, as shown in Fig. 3b. This experimental result is consistent with that observed in the stress-birefringence of 20 at% Yb:YAG, as shown in Fig. 4.

3.3. Dislocation generation and propagation in Yb:YAG

According to the observations in Figs. 2a–c, the growth dislocations may originate from the following sources: (i) dislocations already existing in the seed; (ii) dislocations produced by nucleation at the seed–crystal interface, where some defects such as mechanical damage of the seed end, aggregation of impurity particles and inclusions, and thermal shock stress do exist, as shown in Figs. 2a and b. These dislocations are the main types of source in the as-grown Yb:YAG crystals; (iii) dislocations emerging from the impurity particles and inclusions trapped within the crystal during crystal growth. Comparing Figs. 2a–c, we can see that the propagation direction of the dislocations is perpendicular to the S/L interface and as a result the dislocations mainly center at the periphery of the upper parts. This rule can be explained by the minimum energy principle, since the dislocations take the shortest way and locate in the lowest energy state only when they take this way. Deng [10] found a similar rule in Nd:YAG crystal. Schmidt [11] also found this rule in GGG crystal and calculated the propagating path of dislocations with Klapper theory [12]. Therefore, in order to obtain high-quality Yb:YAG crystal, it is necessary to choose high-quality seeds free from dislocations and grow the initial part of the crystal with high-convex S/L interfaces to eliminate dislocations.

4. Conclusion

The growth defects in [1 1 1]-oriented Czochralski-grown 20 at% Yb:YAG single crystal have been investigated by chemical etching and transmission synchrotron topography. Growth striations, core and dislocations were the main growth defects in Yb:YAG. The etch pits on three low-index faces (1 1 1), (1 1 0) and (2 1 1) have different shapes. The pit pattern on the (1 1 1) face has two shapes, one is triangular, and the other is six-sided. The pit pattern on (2 1 1) is triangular with a tail and the pit pattern on (1 1 0) is a type of distorted rhombus. The dislocations mainly originate from the following sources: (a) dislocations already existing in the seed; (b) dislocations produced by nucleation at the seed–crystal interface, where some defects are present; (c) dislocations emerging from the impurity particles and inclusions trapped within the crystal during crystal growth. Dislocation propagation complies with the rule that it is perpendicular to the solid–liquid interface. Therefore, in order to acquire high-quality crystals of Yb:YAG, it is very important to choose high-quality seeds and S/L interface should be sufficiently convex for eliminating dislocations in the initial growth stage.

Acknowledgements

This work was supported by the National Natural Science foundation of China under Project 69578026 and National 863-416 Foundation of China.

References

[1] R.M. Klbas et al., IEEE J. Quantum Electron. QE-24 (1998) 1605.

[2] T.Y. Fan, IEEE J. Quantum Electron. 29 (1993) 1457.
[3] L.D. Deloach, S.A. Payne, L.L. Chase et al., IEEE J. Quantum Electron. 29 (1993) 1179.
[4] P. Lacovara, H.K. Choi, C.A. Wang et al., Opt. Lett. 16 (1991) 1089.
[5] C. Honninger, I. Johannsen, M. Moser et al., Appl. Phys. B 65 (1997) 523.
[6] P.Z. Yang, P.Z. Deng, J. Xu et al., J. Crystal Growth 216 (2000) 348.
[7] R. Sang, Etching of Crystal Theory, Experiment and Application, North-Holland, Amsterdam, 1987, p. 303.
[8] R.D. Shannon, Acta Crystallogr. Sect A 32 (1976) 751.
[9] A.R. Reinburg, L.A. Riseurg, R.M. Brown et al., Appl. Phys. Lett. 1 (1971) 19.
[10] P.Z. Deng et al., Acta Phys. Siloca 4 (1976) 25.
[11] W. Schmidt, R. Weiss, J. Crystal Growth 43 (1978) 515.
[12] H. Klapper, H. Kuppers, Acta Crystallogr. A 29 (1973) 495.